

The multilayered structure of the human corpus spongiosum

P. De Graaf¹, R. Ramadan¹, E.C. Linssen¹, N.A. Staller¹, A.P.A. Hendrickx^{2*}, G.L.S. Pigot^{3,4}, E.J.H. Meuleman³, M. Bouman^{4,5}, M. Özer^{4,5}, J.L.H.R. Bosch¹ and L.M.O. de Kort¹

¹Department of Urology, ²Department of Medical Microbiology, University Medical Center Utrecht, ³Department of Urology, ⁴Center of Expertise on Gender Dysphoria and ⁵Department of Plastic, Reconstructive and Hand Surgery, VU Medical Center Amsterdam, the Netherlands

*Present address: Foundation Hubrecht Organoid Technology, The Netherlands

Summary. Purpose. Urethral reconstruction is performed in patients with urethral strictures or for correction of congenital disorders. In the case of shortage of tissue, engineered tissue may enhance urethral reconstruction. As the corpus spongiosum (CS) is important in supporting the function of the urethra, tissue engineering of the urethra should be combined with reconstruction of a CS. For that purpose, detailed knowledge of the composition of the CS, more specifically its extracellular matrix (ECM) and vascularization is needed for scaffold design. The objective of this study is to analyze the microarchitecture of the CS through (immuno) histology and scanning electron microscopy (SEM).

Methods. The CS including the urethra of patients undergoing male-to-female genital confirming surgery was harvested. This CS was fixed and processed for either (immuno) histology or for SEM.

Results. Four layers could be distinguished in the CS; first a transition zone from urethra epithelium to a collagen rich layer, which was highly vascularized, followed by a second, elastin rich layer. The third layer was formed by veins, arteries and vascular spaces and the last layer showed the transition from this vascular rich region to the collagen rich tunica albuginea. In this layer collagen bundles intertwined with elastic fibres. In

the CS different components of the ECM were visible and distinguishable.

Conclusion. This study provides novel and detailed information on the microarchitecture of the CS and the distribution of vascularization, which is important for scaffold design in tissue engineering.

Key words: Corpus spongiosum, Urethra, Tissue Engineering, Microscopy, Histology

Introduction

Urethral reconstructive surgery is performed in patients with urethral stricture disease or to correct congenital urethral anomalies such as hypospadias. Urethral stricture is a process of fibrosis that constricts the lumen. Fibrosis can be induced by external trauma or by iatrogenic trauma due to transurethral instrumentation or open surgery, infection or lichen sclerosis (Mundy and Andrich, 2011). Hypospadias is a congenital anomaly of the penis in which the meatus of the urethra is not located at the top of the glans of the penis but more proximally with (partial) absence of the corpus spongiosum (CS) (Baskin, 2000; Baskin and Ebbers, 2006). In hypospadias repair, penile skin, including the prepuce, is used for reconstruction (Baskin and Ebbers, 2006; Snodgrass, 2002). For patients with severe hypospadias or those with complications after primary repair, a 2-stage repair, often with a buccal mucosal graft, is a suitable treatment option (Bracka, 1995).

For treatment of urethral strictures, two types of

Offprint requests to: P. De Graaf, Division Surgical Specialties, Experimental Urology (HP C04.236), University Medical Center Utrecht, P.O. Box 85500, 3508 GA, Utrecht, The Netherlands. e-mail: p.degraaf-4@umcutrecht.nl

DOI: 10.14670/HH-18-022

urethral reconstruction (urethroplasty) exist. First, excision of the fibrotic segment and primary anastomosis, and second substitution urethroplasty using non-urethral tissue (Barbagli et al., 2007). The excision and primary anastomosis procedure achieves excellent cure rates (Micheli et al., 2002; Santucci et al., 2002; Barbagli et al., 2007) but is only feasible for short anterior urethral strictures in the bulbar region. For longer strictures or strictures in the pendular part of the penis, substitution urethroplasty is the preferred method (Mundy and Andrich, 2011).

In addition to buccal mucosa, various other tissue types are used as a substitute, such as skin grafts, bladder mucosa, lingual mucosa and intestinal mucosa (Browne and Vanni, 2017). Unfortunately, tissue grafts have drawbacks such as donor site morbidity, stricture recurrence, the formation of a urethrocutaneous fistula or graft failure such as shrinkage. Most complications are related to a suboptimal blood supply due to the absence of adequate vascular embedding (Palmer et al., 2015). The location of the stricture is a significant determinant of the recurrence rate: urethroplasty in the penile urethra (pars pendulans) has worse outcome compared to a procedure in the bulbar region (pars fixa) (Mangera et al., 2016). Optimizing tissue grafts and adjacent vascularization may improve the long-term outcomes of substitution urethroplasty. Furthermore, patients treated for proximal hypospadias at young age often experience failure of the neo-urethra during adolescence and early adulthood. One of the explanations for this is that at adolescence this neo-urethra fails to keep up with the normal penile and urethral growth, and therefore becomes too short and/or too narrow (Barbagli et al., 2006). In addition sexual activity can mechanically damage the neo-urethra that is not supported by the CS (Yiee and Baskin, 2010).

Penile erection is regulated by blood inflow in the corpora cavernosa and into the CS, although the pressure in the CS is much lower (around one third of the pressure in the corpora cavernosa) (Lue, 2012). The three corpora are expandable, sponge-like structures and the male urethra is an integral part of the CS. The spongy urethra consists of different layers: the (sub)mucosa of the urethra, the spongy vascular tissue and the tunica albuginea corporis spongiosum surrounding the CS (Lue, 2012). In damaged urethra, repair of the urethral epithelial layer only is sufficient if there is a healthy well vascularized CS. However, in failed hypospadias and recurrent urethral stricture cases, usually healthy CS is absent (Lumen et al., 2011). Consequently, vascular supply required for normal growth is lacking as well as the mechanical support during sexual activity. Tissue engineering for urethral reconstruction has been tested mainly in preclinical setting (reviewed by Xue et al., 2016) and sparsely in clinical setting (reviewed by Versteegden et al., 2017). In the latter review it was shown that the state of the CS determines the success of the tissue engineered graft in urethral reconstruction. Therefore regeneration of

urethral tissue combined with accurate restoration of the surrounding CS could improve the results of reconstructive urethral surgery in the case of absence of healthy CS (de Kemp et al., 2015).

Recently, we described a method to visualize the architecture of the CS (Ottenhof et al., 2016). In addition to the architecture, the microarchitecture and more specifically the distribution of extracellular matrix (ECM) and vascular components is important for scaffold design. The aim of the current study was to characterize the CS using different staining methods and microscopy techniques in order to improve knowledge on the microarchitecture of the CS with special emphasis on the extracellular matrix and vascular components.

Material and methods

Material

Penile spongy urethra was collected from patients undergoing male-to-female genital confirming surgery. The use of left-over body material was approved by the medical ethics board of the VUmc. All four included patients gave written informed consent. The left-over material was processed in two ways: directly fixed in formaldehyde and embedded in paraffin, or transported in phosphate buffered saline (PBS) on ice before fixing in glutaraldehyde and subsequent preparing for SEM.

Antibodies

Antibodies used are listed here: Collagen I from Abcam (ab138492), collagen III from Southern Biotech (1330-01), collagen IV was from Merck (Ab769), collagen VI was from Sigma (Prestige antibody, HPA019142). Laminin was from Sigma (L-9393), von Willebrand Factor (vWF) and CD31 were from DAKO (Glostrup, Denmark, a0082 and JC70A resp.), V/E-cadherin was from Millipore (Amsterdam, the Netherlands, clone BV9). Secondary and tertiary antibodies coupled to horse radish peroxidase (HRP) were purchased at DAKO (Glostrup, Denmark), except Brightvision goat anti rabbit HRP and Brightvision goat anti mouse HRP which were from ImmunoLogic (Duiven, the Netherlands)

Scanning electron microscopy (SEM)

Tissue blocks were fixed for 15 minutes in 1% (v/v) glutaraldehyde (Sigma) in phosphate buffered saline (PBS) at room temperature (RT). Samples were washed with PBS to remove excess fixative and were subsequently serially dehydrated by consecutive 30 minute incubations in 5 ml of 10% (v/v), 25% (v/v) and 50% (v/v) ethanol-PBS, 75% (v/v) and 90% (v/v) ethanol-H₂O, and 100% ethanol (2x), followed by 50% ethanol-hexamethyldisilazane (HMDS) and 100% HMDS (Sigma). The samples were removed from the 100% HMDS and air-dried overnight at RT. After

Multilayered corpus spongiosum

overnight evaporation of HMDS, samples were mounted onto 12 mm specimen stubs (Agar Scientific) and coated with gold to 1 nm using a Quorum Q150R sputter coater at 20 mA prior to examination with a Phenom PRO Table-top scanning electron microscope (PhenomWorld, Eindhoven, The Netherlands). Collagen and elastin fibre structure has been previously described and SEM images have been published (Hsu et al., 1994).

(Immuno) histochemistry

For morphological analysis 3 μ m paraffin-embedded spongy urethra sections were stained using a DAKO ArtisanTM Staining System (Glostrup, Denmark). For staining of the ECM two cassettes were used, the Elastin (AR163) and Masson's Trichrome (AR173). In the Elastin staining, elastin fibres and nuclei are stained black, collagen is red and all other tissue elements are stained yellow. As for the Masson's Trichrome staining, collagen is seen in blue, nuclei in black and the red colour represents muscles, cytoplasm and keratin. Alcian Blue/Picosirius Red staining was performed on on 3 μ m paraffin-embedded spongy urethra sections. In short, sections were deparaffinized and rinsed in water, followed by a 5min staining step with Weigerts Haematoxylin solution, after staining, samples were developed under running tap water for 10min, rinsed in distilled water and subsequently stained with Alcian Blue solution for 30 min, rinsed in tap water and stained in Picosirius Red solution for 1h. Sections were rinsed in 0.01M HCl till clear and dehydrated and embedded. Acidic GAGs are stained in blue, collagens in red, cytoplasm in yellow.

Immunostainings were performed on 3 μ m paraffin-embedded spongy urethra sections. In short, sections were deparaffinized and treated with PO block for 15 minutes and antigen retrieval was performed by incubation at 100°C in Citrate/HCl buffer for 20 minutes. For collagen I antigen retrieval was performed by a combination of pronase treatment (Roche, 11459643001, 1 mg/ml in PBS) for 30 minutes at 37°C and 20 minutes incubation at 100°C in Tris-EDTA buffer pH 8.5. Sections were blocked in BSA for 30 minutes, followed by incubation with primary antibody for 1-2h at RT. After washing, secondary antibody was applied for 30 min, followed either by a 3rd antibody for 30 minutes to enhance signal or directly proceeded to the Nova RED substrate kit for Peroxidase (Vector, SK-4800) for development of the signal (brown staining). All sections were counterstained with hematoxyline. Four different collagen types were used (collagen I, III, IV and VI), Laminin and three different markers for endothelial cells were used: CD31 (cluster of differentiation 31, on surface of blood cells as platelets and also in endothelial cell intercellular junctions), vWF (von Willebrand factor, blood glycoprotein that is present in endothelial cells to enable platelet adhesion) and V/E-cadherin (vascular endothelial cadherin, adherence junction protein of endothelial cells for

maintenance of barrier function).

Results

Histochemical staining of extracellular matrix components

To study the architecture of the CS in molecular detail, two histochemical stains were performed on human CS sections for visualization of elastin fibres and collagen (Fig. 1).

Both stainings suggested a multi-layered structure of the CS (Fig. 1A). Four distinct layers were found; 1) the interphase between the urethral epithelium and the CS (Fig. 1B), 2) an elastin dense region (Fig. 1C) followed by 3) vascularised spaces (Fig. 1D), and 4) the interphase between the CS and the tunica albuginea (TA) (Fig. 1E). The interphase between the urethral epithelium and the CS (Fig. 1B) was rich in collagen and had less elastin fibres than the next layer, the elastin dense region (Fig. 1C). There were few vascular structures and glands in this interphase, visible in yellow with the Elastin staining (Fig. 1B left panel) and in red with Masson's Trichrome staining (Fig. 1B right panel).

Deeper in the CS, there was a second thin layer, mainly consisting of elastic fibres (Fig. 1C). The third layer was the most voluminous of the layers of the CS, and gave the tissue its spongy characteristic. This layer was formed by arteries, veins and other vascular spaces (Fig. 1D). Left panel shows a vascular space surrounded by smooth muscle cell lining, which was encapsulated within a thin layer of elastin (Fig. 1D left). The same section stained with Masson's Trichrome is presented in the right panel (Fig. 1D right). It illustrates collagen infiltration between the smooth muscle cells. The last layer, which constituted the interphase between the CS and the TA, displayed collagen bundles in a wave-like structure intertwined with short elastic fibres (Fig. 1E). This panel also showed enclosed glandular structures.

Based on the Masson's Trichrome staining we further analyzed the collagen types in the CS. Type I and III form collagen bundles, type IV is part of the basal membrane of vascular structures and type VI is involved in microfibrils. Figure 2 shows an overview of the different collagen stainings, collagen I (Fig. 2A,B) and III (Fig. 2C,D) overlap in distribution, both are stained throughout all layers of CS, with an enrichment close to the urethral epithelium. Collagen IV and VI are also present throughout all layers, but differently enriched around vessels and vascular spaces (Fig. 2E-H). Detection of Collagen I required a pronase treatment for antigen retrieval, this affected the urethral epithelial integrity (Fig. 2A,B). Another component of the extracellular matrix is laminin, which is an elastic component of basement membranes. In Figure 3 the distribution of laminin is shown. The vascular spaces (indicated with an asterisk) are surrounded by laminin, as well as the microvascular network close to the urethral epithelium (Fig. 3A,B). Lastly a non-protein

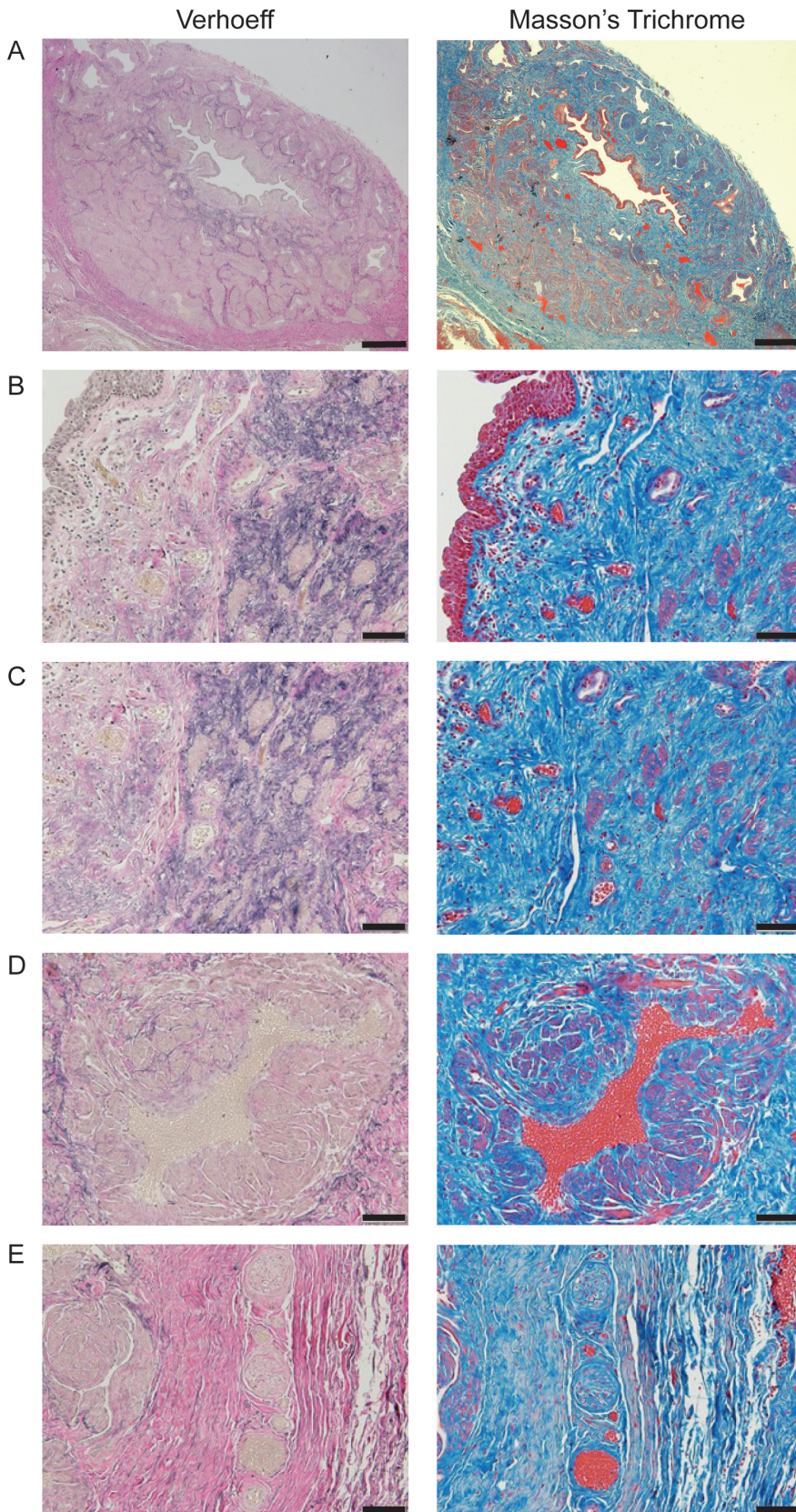


Fig. 1. Staining of extracellular components in the CS. Elastin staining (left panel) and Masson's Trichrome staining (right panel). For explanation of the colors see materials and methods. **A.** Overall view of the urethra and CS. **B.** Interphase between the urethra epithelium and the CS. **C.** Elastin dense region. **D.** Vascular space surrounded by smooth muscle. **E.** Interphase between spongy vascular region and tunica albuginea. Scale bars: A, 1 mm; B-E, 200 μ m.

Multilayered corpus spongiosum

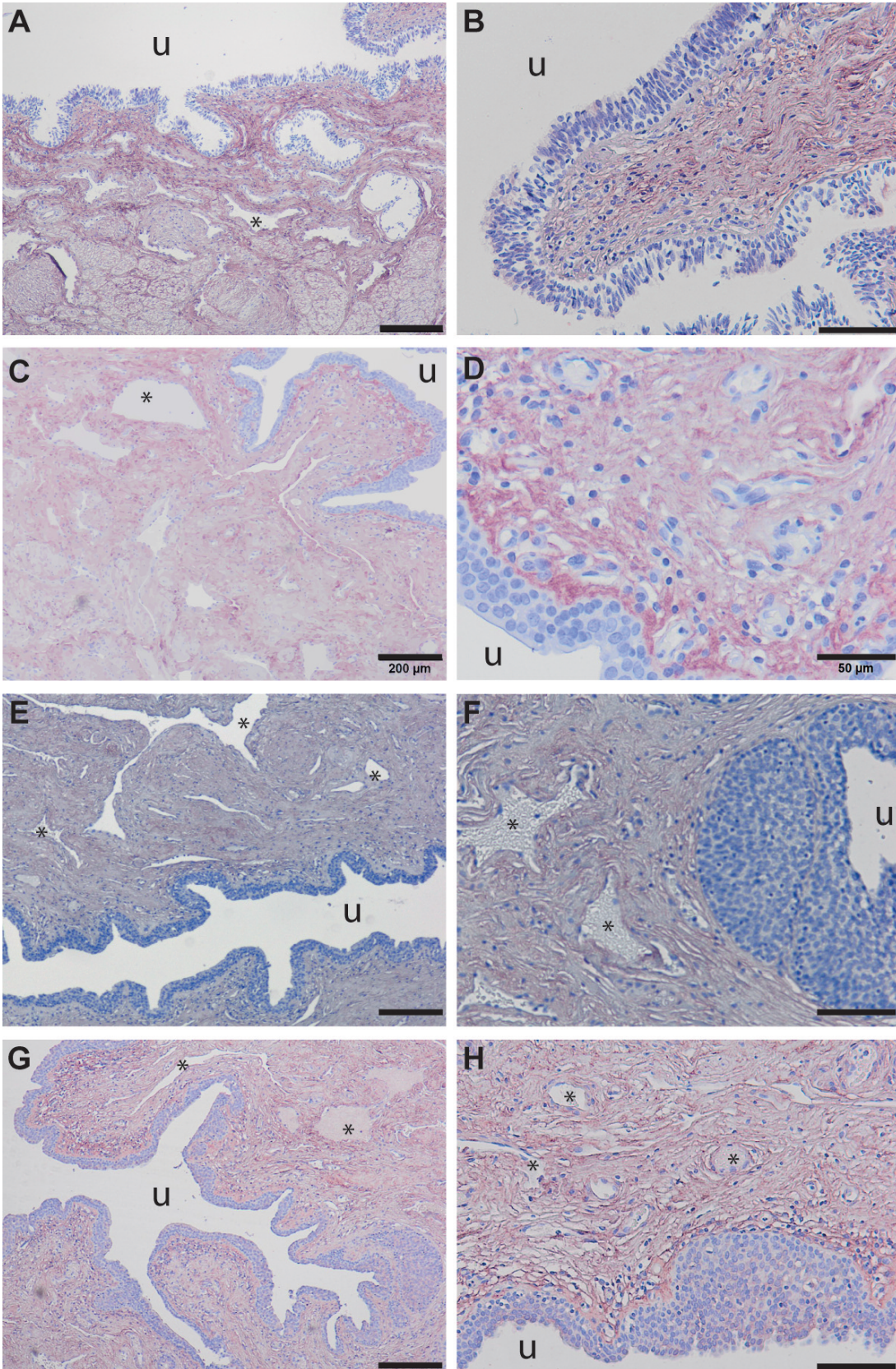


Fig. 2. Collagen type analysis of human urethra and CS. u represents urethral lumen, * indicates vascular spaces.
A. Collagen I staining.
B. Collagen I staining.
C. Collagen III staining.
D. Collagen III staining.
E. Collagen IV staining.
F. collagen IV staining.
G. collagen VI staining.
H. collagen VI staining.
 Scale bars: A, C, E, G, 200 μm; B, F, H, 100 μm; D, 50 μm.

component of the ECM was analyzed, the specific carbohydrate polymers making up the glycosaminoglycans (GAGs). These negatively charged molecules link the growth factors and the ECM and are detected with alcian blue staining. Figure 3 shows the presence of GAGs mainly inside the vascular spaces (Fig. 3D), staining is sparsely found in the urethra or in urethral glands (Fig. 3C).

Ultrastructural analysis of the multi-layered CS

In addition to histochemistry, SEM was used to investigate the microscopic architecture of the CS (Fig. 4). In the human CS four different layers could be distinguished. Figure 4A shows an overview of the human urethral lumen. The cells are tightly bound and form a flat sheet with a few exceptions of loose cells. At

a higher magnification, a honeycomb-like structure was recognized: the urethral cells have a pentagonal or hexagonal geometry (Fig. 4B). The interphase between the urethra and the CS is shown in Fig. 4C. On the right side of the image are the urethral cells and on the left side are fibrous structures surrounding the urethral epithelium, which constitute the connective tissue between the urethra and the CS. A closer look at the fibres showed collagen bundles intertwined with rope-like elastin fibres with short thin fibrils in between (Fig. 4D).

Analysis of vasculature in the CS

Staining with three different markers for endothelial cells CD31 (Fig. 5A-C), vWF (Fig. 5D,E) and V/E-cadherin (Fig. 5F) showed microvasculature close to the

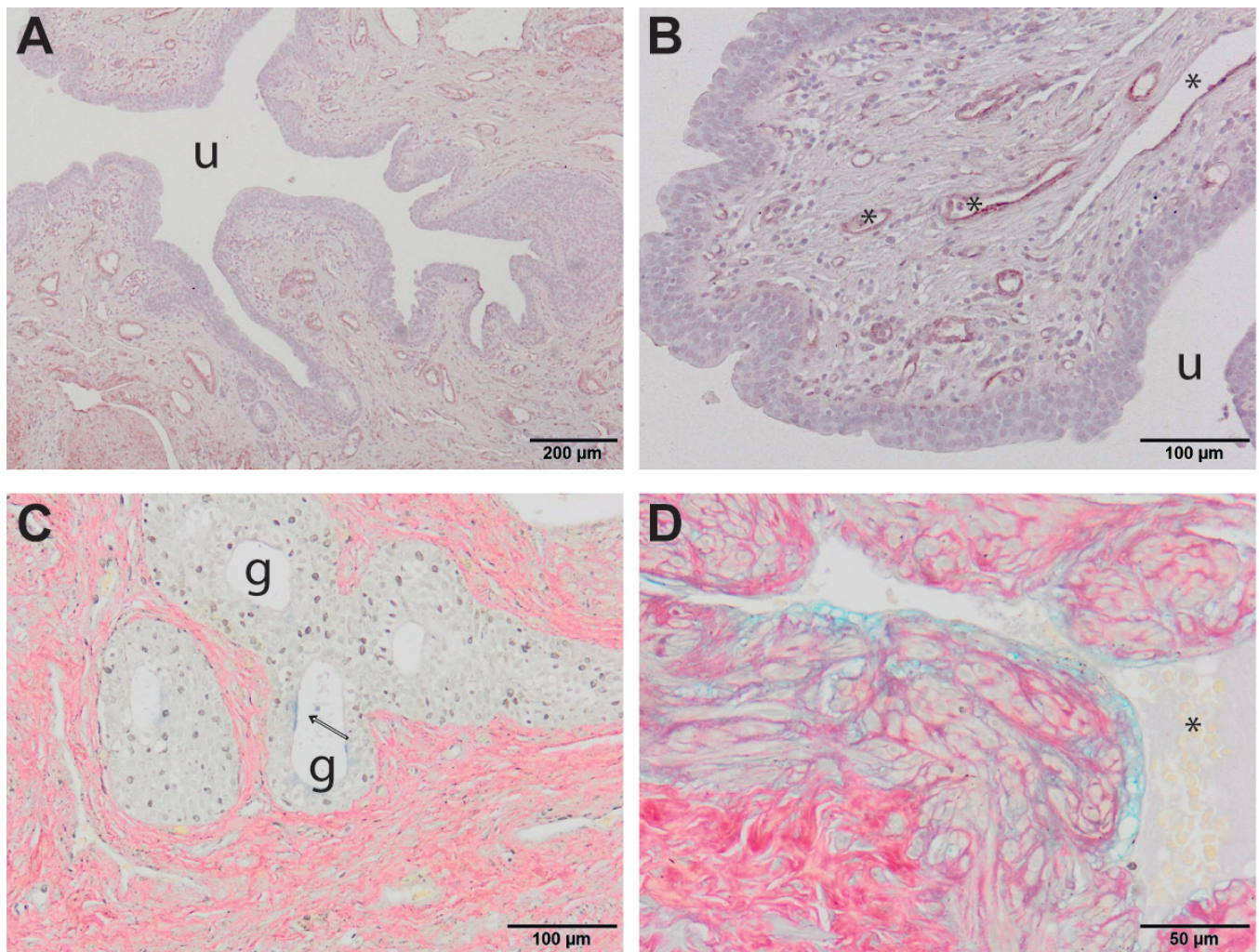


Fig. 3. ECM analysis of human urethra and CS. g represents urethral glands, u represents urethral lumen, * indicates vascular spaces. **A.** Laminin staining. **B.** Laminin staining. **C.** Picrosirius Red/Alcian blue staining, in red collagens, in blue GAGs. Arrow indicates GAGs inside urethral glands. **C, D.** GAGs on the inside of a vascular space. Scale bars: A, 200 μm ; B, C, 100 μm ; D, 50 μm .

Multilayered corpus spongiosum

urethral epithelial cell lining (Fig. 5B,E, urethra is indicated with an "u") and larger blood vessels such as arteries or veins in peripheral spongy tissue, in between the vascular spaces. Positive signal of the vascular markers on the luminal side of vascular spaces (indicated with an asterisk) illustrated that a thin line of

endothelial cells covered these cavities (Fig. 5C,E,F).

The endothelial lining in the CS was further analyzed (Fig. 6). Figure 6A shows a SEM analysis of a small artery with a close up in Fig. 6B. The endothelium had a cobblestone-like tight lining. Figure 6C shows a vein in the middle of a number of vascular spaces, from

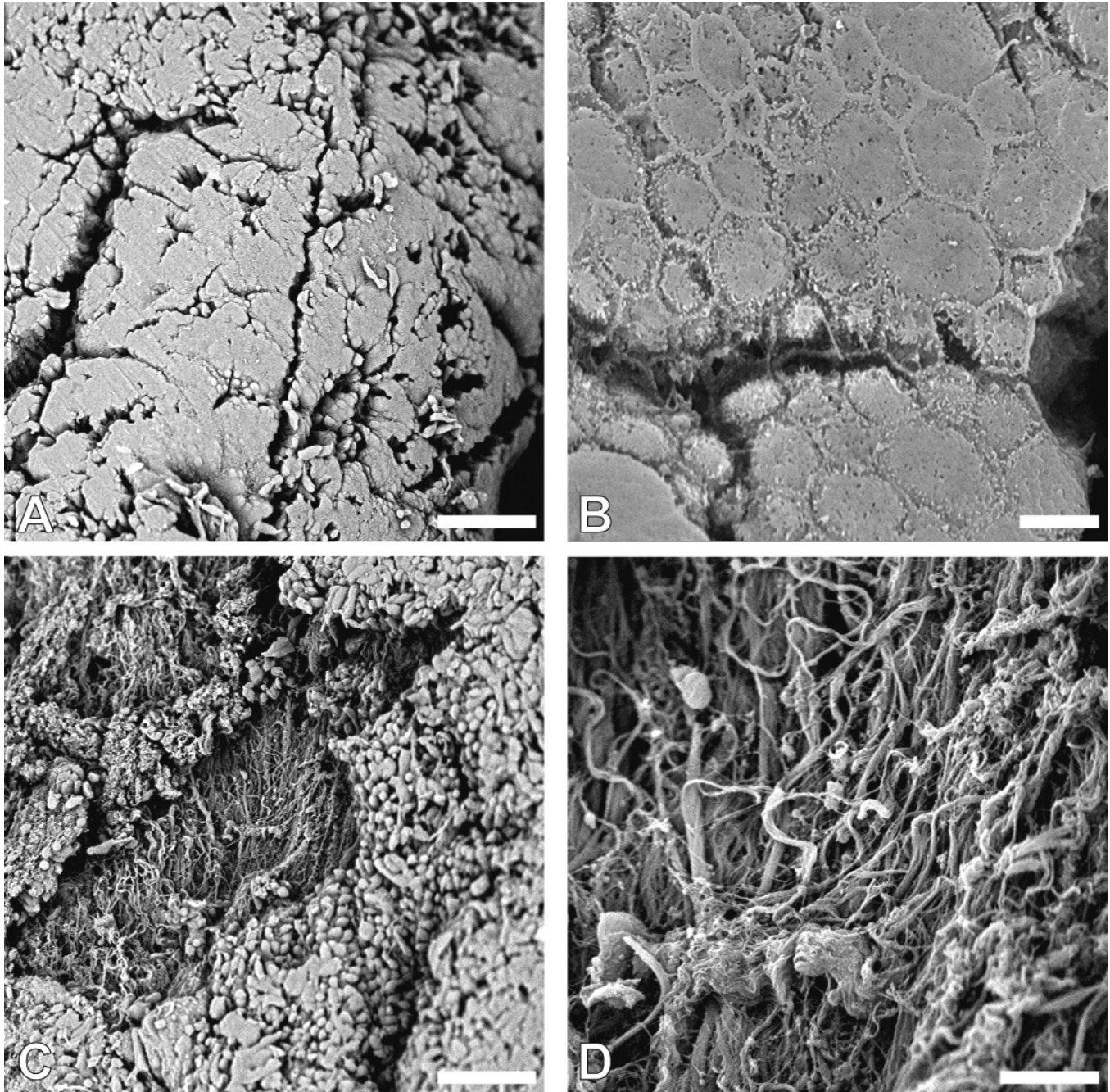


Fig. 4. SEM analysis of human urethra and CS. **A.** Human urethra. **B.** Urethral cell close-up, honeycomb-like structure. **C.** Interphase between urethra and the CS. **D.** Intertwined collagen bundles and elastin rope-like fibres. Scale bars: A, C, 50 μm ; B, 5 μm ; D, 10 μm .

the spongy region of the CS. At higher magnification similar endothelial lining was shown in the vascular spaces (compare Fig. 6B with 6D). This is consistent with the data shown in Fig. 5.

Summary of results

We found that the CS consists of distinct layers with distinct composition, both in cellular and extracellular components. Four layers could be distinguished in the CS; from the urethral lumen first a highly vascularized, collagen rich layer is followed by a second, elastin rich layer. The third layer was formed of veins, arteries and vascular spaces, covered by endothelium and the last outer layer was the transition from this vascular rich region to the collagen rich tunica albuginea. In this layer collagen bundles appeared in a wave-like structure intertwined with short elastic fibres.

Discussion

Here we described the microarchitecture of the human corpus spongiosum. Macroscopic analysis of the CS in both flaccid and erect penises has been previously published (Ottenhof et al., 2016) and literature on the microarchitecture of the urethra (Zecchi-Orlandini et al., 1988) and the cavernosal corporal tissue (Goldstein and Padma-Nathan, 1990) is available. However, we are the first to describe the microarchitecture of the CS with

special emphasis on the ECM and the vasculature. Using both histological and immunohistological techniques combined with ultrastructural analysis by electron microscopy we could identify distinct layers in the spongy urethra (the integral combination of the urethra and the CS). The aim of our study was to gain insight into the structure of the spongy urethra. This insight is necessary for tissue engineering purposes, and thus generating potential solutions for local tissue shortage in urethral reconstruction.

As mentioned above, the CS consists of layers with distinct composition, both in cellular and extracellular components, each of which represents a specific function that adds to the overall tissue homeostasis. Four layers could be distinguished in the CS; from the urethral lumen first a highly vascularized, collagen rich layer, than a second, elastin rich layer followed by a third layer formed of veins, arteries and vascular spaces. In the last layer the vascular rich region transits to the collagen rich tunica albuginea, here collagen bundles are intertwined with short elastic fibres in a wave-like structure. Collagens I and III were enriched in the layer close to the urethral epithelium, whereas collagens IV, VI and laminin were enriched around vessels, arteries and vascular spaces. GAGs were identified by alcian blue staining in the vascular spaces. For more detailed analysis of GAGs in the penis we refer to Goulas et al. (2000).

The different composition of the layers probably

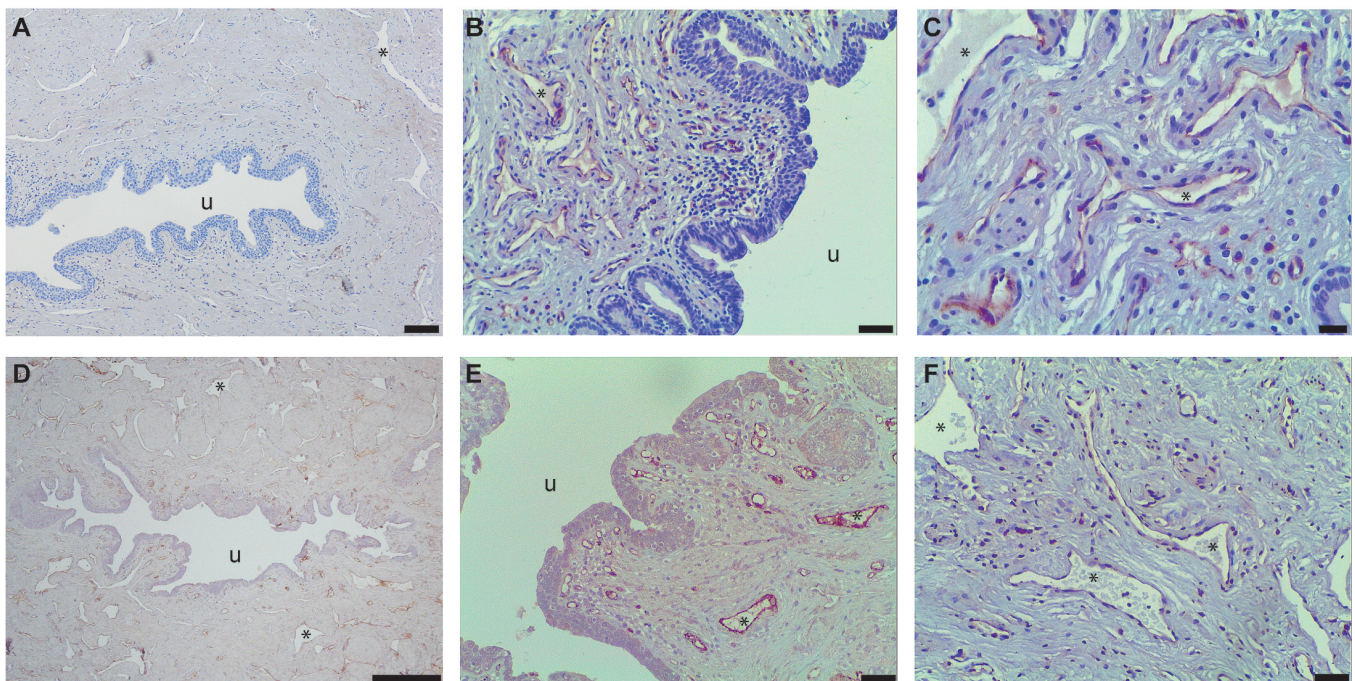


Fig. 5. Endothelial marker staining of human CS. u represents urethral lumen, * indicates vascular spaces, red-brown staining represents positive signal **A.** CD31 staining. **B.** CD31 staining. **C.** CD31 staining. **D.** vWF staining. **E.** vWF staining. **F.** VE-cadherin staining. Scale bars: A, 100 μm ; B, E, F, 25 μm ; C, 10 μm ; D, 500 μm .

Multilayered corpus spongiosum

represents a specific function. The highly vascularized layer with microvessels close to the epithelium surrounding the urethra presumably makes up a vascular bed for the urethra, providing an excellent supply of oxygen and nutrition for the urethral epithelial cells. These vessels are embedded in collagen providing

firmness. The spongy region was shown to contain main vessels and microvessels but also open vascularized spaces that contribute to the swelling during erection, thereby preventing compression of the urethra. It has been shown previously that the vascular spaces in the corpus cavernosum (CC) are lined with endothelium

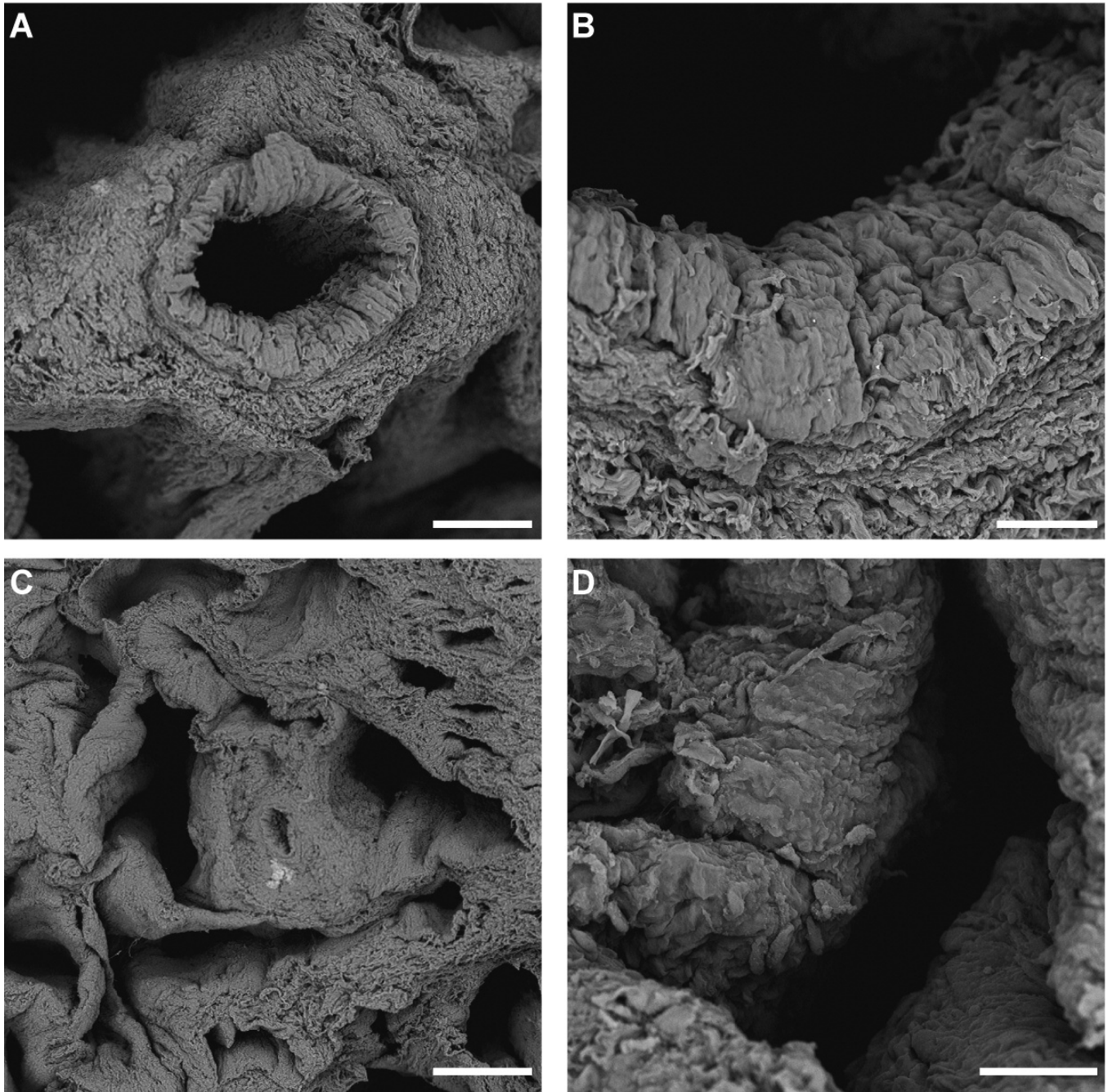


Fig. 6. SEM analysis of vascular structures in the CS. **A.** Artery in spongy tissue. **B.** Lining of artery in spongy tissue. **C.** vascular open spaces with vessel in the center. **D.** Lining of the vascular spaces in the spongy tissue. Scale bars: A, 100 μm ; B, 30 μm ; C, 200 μm ; D, 20 μm .

(Wessells et al., 2004). We show in this study that the lining of the vascular spaces in the CS shares characteristics with other vascular structures in the CS (Figs. 5, 6).

The elastic layer slightly further away from the lumen probably gives the tissue the controlled flexibility needed for erection and micturition, but in combination with collagen also adds strength to the structure thereby avoiding damage of the tissue. In humans the concentration of elastic fibres is highest in the glans penis, followed by the CS and the CC (Hsu et al., 1994). A linear increase of elastin content in the spongy urethra has been shown when voiding function firstly occurs during fetal development, suggesting that elastin has a function during voiding and that the pressure caused by fetal micturition is of importance for the development of a normal male fetal urethra (Bastos et al., 2004). Animal studies have shown that reduced elastin protein content and less elastin fibres in the CC is associated with erectile dysfunction and infertility (Hidalgo-Tamola et al., 2011; Wood et al., 2009). In these models the CS was not analyzed.

Tissue engineering of corporal tissue has been described in a preclinical setting (de Vocht et al., 2018; Kajbafzadeh et al., 2017a), with the main focus on CC, only three studies described TE CS for urethral reconstruction (Feng et al., 2010, 2011; Kajbafzadeh et al., 2017b). Knowledge of the CS microarchitecture and the distribution of extracellular matrix and vascular components will help to design a stable environment for the support of a tissue engineered urethral epithelium but also to add proper communication between cells and their surroundings, resulting in a reduction of graft failure. Ideally, an engineered graft for urethral reconstruction will consist of the same layers as the native spongy tissue. Vascularization of the graft is essential, to prevent fibrosis and necrosis. Elasticity is important to regulate the urethral lumen: during erection the urethra should be open, elastin is involved in closure after detumescence. In addition, elastin seems to have a function during voiding as shown during fetal development (Bastos et al., 2004). The spongy layer fills up with blood during erection and pressure builds up because of the firm last layer of collagen intertwined with elastin fibres. Together these two layers generate a sort of airbag for the urethra, protecting its lumen from compression during sexual activity (Yiee and Baskin, 2010).

Whether all the distinct layers of the CS are required for an engineered graft remains to be shown in future preclinical experiments. Perhaps a homogenous graft, with all the different properties (vascularized, elastic and spongy) with a firm tunica surrounding the graft will suffice.

Limitations

A limitation of this study is that the analysis is performed in CS of transgender women. Given the

privacy of the patients full medical history is unknown, however, it is safe to assume that these individuals have been exposed to cross sex hormones (anti-androgen) therapy before genital confirmation surgery. This therapy, depending on the onset, can influence the size of the genitals, and may influence the composition of the extracellular matrix. Androgens are known to affect development, growth and maintenance of penile erectile tissue (Traish and Kim, 2005). We have chosen this material because initial experiments using cadaveric samples show degenerating epithelium in the urethra and endothelium in the corporal tissue (results not shown). Human spongy urethra from potent young men is not readily available. Animal specimens are not a valid alternative option as humans have a unique penile anatomy (Hsieh et al., 2012).

Another limitation is that this study is merely focused on collagens, elastin and laminin, whereas the extracellular matrix consists of more components. Future work will seek to understand the exact composition of the ECM. For this complete characterization of the extracellular matrix a more unbiased approach like genomics or proteomics should be performed.

Conclusion

In conclusion, we have shown that the human CS is a multilayered structure with characteristic composition of the different layers. This is the first study that shows the microarchitecture of the CS with special emphasis on the distribution of collagen, elastin and vasculature. This information is essential for scaffold design in tissue engineering of the corpus spongiosum. Future experiments are needed to understand whether this layered structure is required for proper function or if a homogenous tissue with similar characteristics (vascularized, elastic and spongy) can be used to reconstruct urethras in hypospadias or complicated stricture disease.

Acknowledgments. We would like to thank Natasja Carpitella, Pieter Lindenbergh, Franziska Zügel and Krista den Ouden for technical assistance, Lian Elfering for help in obtaining the human tissue samples and Marie-Anne van Stam for help creating the figures.

References

- Barbagli G., De Angelis M., Palminteri E. and Lazzeri M. (2006). Failed hypospadias repair presenting in adults. *Eur. Urol.* 49, 887-894.
- Barbagli G., De Angelis M., Romano G. and Lazzeri M. (2007). Long-term followup of bulbar end-to-end anastomosis: a retrospective analysis of 153 patients in a single center experience. *J. Urol.* 178, 2470-2473.
- Baskin L.S. (2000). Hypospadias and urethral development. *J. Urol.* 163, 951-956.
- Baskin L.S. and Ebberts M.B. (2006). Hypospadias: anatomy, etiology, and technique. *J. Pediatr. Surg.* 41, 463-472.
- Bastos A.L., Silva E.A., Silva Costa W. and Sampaio F.J. (2004). The

Multilayered corpus spongiosum

- concentration of elastic fibres in the male urethra during human fetal development. *BJU Int.* 94, 620-623.
- Bracka A. (1995). A versatile two-stage hypospadias repair. *Br. J. Plast. Surg.* 48, 345-352.
- Browne B.M. and Vanni A.J. (2017). Use of alternative techniques and grafts in urethroplasty. *Urol. Clin. North Am.* 44, 127-140.
- de Kemp V., de Graaf P., Fledderus J.O., Ruud Bosch J.L. and de Kort L.M. (2015). Tissue engineering for human urethral reconstruction: systematic review of recent literature. *PLoS One* 10, e0118653.
- de Vocht D., de Kemp V., Iltas J.D., Bosch J., de Kort L.M.O. and de Graaf P. (2018). A systematic review on cell-seeded tissue engineering of penile corpora. *J. Tissue Eng. Regen. Med.* 12, 687-694.
- Feng C., Xu Y.M., Fu Q., Zhu W.D., Cui L. and Chen J. (2010). Evaluation of the biocompatibility and mechanical properties of naturally derived and synthetic scaffolds for urethral reconstruction. *J. Biomed. Mat. Res. Part A* 94, 317-325.
- Feng C., Xu Y.M., Fu Q., Zhu W.D. and Cui L. (2011). Reconstruction of three-dimensional neourethra using lingual keratinocytes and corporal smooth muscle cells seeded acellular corporal spongiosum. *Tissue Eng. Part A* 17, 3011-3019.
- Goldstein A.M. and Padma-Nathan H. (1990). The microarchitecture of the intracavernosal smooth muscle and the cavernosal fibrous skeleton. *J. Urol.* 144, 1144-1146.
- Goulas A., Papakonstantinou E., Karakioulakis G., Mirtsou-Fidani V., Kalinderis A. and Hatzichristou D.G. (2000). Tissue structure-specific distribution of glycosaminoglycans in the human penis. *Int. J. Biochem. Cell Biol.* 32, 975-982.
- Hidalgo-Tamola J., Luttrell I., Jiang X., Li D., Mechem R.P. and Chitale K. (2011). Characterization of erectile function in elastin haploinsufficient mice. *J. Sex Med.* 8, 3075-3085.
- Hsieh C.H., Liu S.P., Hsu G.L., Chen H.S., Molodsky E., Chen Y.H. and Yu H.J. (2012). Advances in understanding of mammalian penile evolution, human penile anatomy and human erection physiology: clinical implications for physicians and surgeons. *Med. Sci. Monit.* 18, RA118-125.
- Hsu G.L., Brock G., von Heyden B., Nunes L., Lue T.F. and Tanagho E.A. (1994). The distribution of elastic fibrous elements within the human penis. *Br. J. Urol.* 73, 566-571.
- Kajbafzadeh A.M., Abbasioun R., Sabetkish N., Sabetkish S., Habibi A.A. and Tavakkolatabassi K. (2017a). In vivo human corpus cavernosum regeneration: fabrication of tissue-engineered corpus cavernosum in rat using the body as a natural bioreactor. *Int. Urol. Nephrol.* 49, 1193-1199.
- Kajbafzadeh A.M., Abbasioun R., Sabetkish S., Sabetkish N., Rahmani P., Tavakkolatabassi K. and Arshadi H. (2017b). Future prospects for human tissue engineered urethra transplantation: Decellularization and recellularization-based urethra regeneration. *Ann. Biomed. Eng.* 45, 1795-1806.
- Lue T.F. (2012). Physiology of penile erection and pathophysiology of erectile dysfunction. In: *Campbell-Walsh urology 10th edn.* Elsevier Saunders, Philadelphia. pp 699-720.
- Lumen N., Hoebeke P., Deschepper E., Van Laecke E., De Caestecker K. and Oosterlinck W. (2011). Urethroplasty for failed hypospadias repair: a matched cohort analysis. *J. Pediatr. Urol.* 7, 170-173.
- Mangera A., Osman N. and Chapple C. (2016). Evaluation and management of anterior urethral stricture disease. *F1000Res* 5, 153.
- Micheli E., Ranieri A., Peracchia G. and Lembo A. (2002). End-to-end urethroplasty: long-term results. *BJU Int.* 90, 68-71.
- Mundy A.R. and Andrich D.E. (2011). Urethral strictures. *BJU Int.* 107, 6-26.
- Ottenhof S.R., de Graaf P., Soeterik T.F., Neeter L.M., Zilverschoon M., Spinder M., Bosch J.L., Bleys R.L. and de Kort L.M. (2016). Architecture of the corpus spongiosum: An anatomical study. *J. Urol.* 196, 919-925.
- Palmer D.A., Buckley J.C., Zinman L.N. and Vanni A.J. (2015). Urethroplasty for high risk, long segment urethral strictures with ventral buccal mucosa graft and gracilis muscle flap. *J. Urol.* 193, 902-905.
- Santucci R.A., Mario L.A. and McAninch J.W. (2002). Anastomotic urethroplasty for bulbar urethral stricture: analysis of 168 patients. *J. Urol.* 167, 1715-1719.
- Snodgrass W.T. (2002). Tubularized incised plate (TIP) hypospadias repair. *Urol. Clin. North Am.* 29, 285-290.
- Traish A. and Kim N. (2005). The physiological role of androgens in penile erection: regulation of corpus cavernosum structure and function. *J. Sex. Med.* 2, 759-770.
- Versteegden L.R., de Jonge P.K., Int'Hout J., van Kuppevelt T.H., Oosterwijk E., Feitz W.F., de Vries R.B. and Daamen W.F. (2017). Tissue engineering of the urethra: A systematic review and meta-analysis of preclinical and clinical studies. *Eur. Urol.* 72, 594-606.
- Wessells H., King S.H., Schmelz M., Nagle R.B. and Heimark R.L. (2004). Immunohistochemical comparison of vascular and sinusoidal adherens junctions in cavernosal endothelium. *Urology* 63, 201-206.
- Wood H.M., Lee U.J., Vurbic D., Sabanegh E., Ross J.H., Li T. and Damaser M.S. (2009). Sexual development and fertility of Lox11-/- male mice. *J. Androl.* 30, 452-459.
- Xue J.D., Gao J., Fu Q., Feng C. and Xie H. (2016). Seeding cell approach for tissue-engineered urethral reconstruction in animal study: A systematic review and meta-analysis. *Exp. Biol. Med.* 241, 1416-1428.
- Yiee J.H. and Baskin L.S. (2010). Penile embryology and anatomy. *Sci. World J.* 10, 1174-1179.
- Zecchi-Orlandini S., Gulisano M., Orlandini G.E. and Holstein A.F. (1988). Scanning electron microscopic observations on the epithelium of the human spongy urethra. *Andrologia* 20, 132-137.